

Atomic Landau-Zener Tunneling in Fourier-Synthesized Optical Lattices

Tobias Salger, Carsten Geckeler, Sebastian Kling, and Martin Weitz

Institut für Angewandte Physik, Universität Bonn, Wegelerstr. 8, D-53115 Bonn, Germany

(Received 13 July 2007; published 6 November 2007)

We report on an experimental study of quantum transport of atoms in variable periodic optical potentials. The band structure of both ratchet-type asymmetric and symmetric lattice potentials is explored. The variable atom potential is realized by superimposing a conventional standing wave potential of $\lambda/2$ spatial periodicity with a fourth-order multiphoton potential of $\lambda/4$ periodicity. We find that the Landau-Zener tunneling rate between the first and the second excited Bloch band depends critically on the relative phase between the two spatial lattice harmonics.

DOI: [10.1103/PhysRevLett.99.190405](https://doi.org/10.1103/PhysRevLett.99.190405)

PACS numbers: 03.75.Lm, 32.80.Pj, 42.50.Vk

Transport properties of quantum objects subject to a periodic potential are determined by the particle's band structure. The energy spectrum here splits into continuous energy bands separated by band gaps. For example, the more than 20 orders of magnitude difference in electrical conductivity between an insulator and a good conductor thus finds a natural physical explanation [1]. In recent years, atoms confined in periodic optical potentials, so called optical lattices, have developed a powerful tool for the observation of effects known or predicted in solid state physics [2]. So far, the band structure has been exploited only for sinusoidal lattice potentials, as can be realized with the ac Stark shift of optical standing waves. In remarkable experiments with such standing wave lattices, Bloch oscillations and Landau-Zener transitions have been observed [3–5].

Here we report on experiments studying the band structure of optical lattices with variable inversion symmetry and shape, as a step towards simulating the variety of potential forms that nature provides us in the system of electrons in natural crystals. The used potentials are realized by superimposing a conventional standing wave lattice of $\lambda/2$ spatial periodicity with a $\lambda/4$ periodicity lattice realized using the dispersion of higher order Raman transitions. By varying the phase between the two spatial harmonics, symmetric and ratchet-type asymmetric lattice potentials are realized, which exhibit a different band structure. We experimentally demonstrate that the strength of interband transitions for an atomic Bose-Einstein condensate depends on the shape of the lattice potential.

Before proceeding, let us point out that in semiconductor heterostructures effects of the inversion symmetry of quantum wells have been studied using magnetotransport [6]. In the area of atomic physics, directed transport has been achieved in driven ratchet systems with the temporal symmetry broken by dissipative processes [7]. Further, in theoretical works, atom transport has been studied in periodic double well systems [8]. Let us begin by describing our calculations of the band structure in a Fourier-synthesized atom potential realized by superimposing

two lattice potentials of spatial periodicities $\lambda/2$ and $\lambda/4$:

$$V(z) = \frac{V_1}{2} \cos(2kz) + \frac{V_2}{2} \cos(4kz + \varphi), \quad (1)$$

where V_1 and V_2 denote the potential depths of the two lattice harmonics, respectively, and φ the relative phase. According to Bloch's theory [9], the band structure of the periodic potential can be derived by solving the eigenvalue equation $M c_l^q = E_q^{(n)} c_l^q$, where the quasimomentum q conventionally is restricted to the first Brillouin zone: $-\hbar k < q < \hbar k$. Here we search for the eigenenergies $E_{q(n)}$ of the eigenstates $|n, q\rangle = \sum_l c_l^q e^{i2lkz}$ using the coupling matrix M with elements $M_{jj} = (2l\hbar k + q)^2/2m$, $M_{j,j+1} = M_{j+1,j}^* = V_1/4$, and $M_{j,j+2} = M_{j+2,j}^* = V_2/4 e^{i\varphi}$, where the index n denotes the band number. The matrix can be readily diagonalized. For the lattice potential of Eq. (1), Fig. 1 shows a spatial lattice potential (left) and the corresponding band structure (right) for different values of the relative phase φ of the two spatial lattice harmonics. It is clearly visible that the gap between the first and second excited band is strongly dependent on the value of the relative phase, while no such significant modification of the splitting between the other shown bands is visible. Physically, the variation of this splitting on the relative phase of the lattice harmonics can be understood by the interference of the second order Bragg scattering amplitude of the standing wave potential of periodicity $\lambda/2$ with the first order Bragg scattering amplitude of the $\lambda/4$ periodicity multiphoton lattice potential, which both contribute to this band gap. In the limit of a very shallow lattice with the four-photon contribution being a small perturbation, i.e., $V_2 \ll V_1 \ll E_r$ (where $E_r = \hbar^2 k^2/2m$ denotes the atomic recoil energy), the size of this band gap is determined by the simple analytical expression $|V_1^2/8E_r + e^{i\varphi} V_2|$, which directly shows the two interfering contributions of coupling Rabi frequencies arising from different lattice harmonics. For larger potential values, higher order corrections come into play, but by numerical diagonalization of the coupling matrix M , the band structure for arbitrary potential values is readily determined. The band

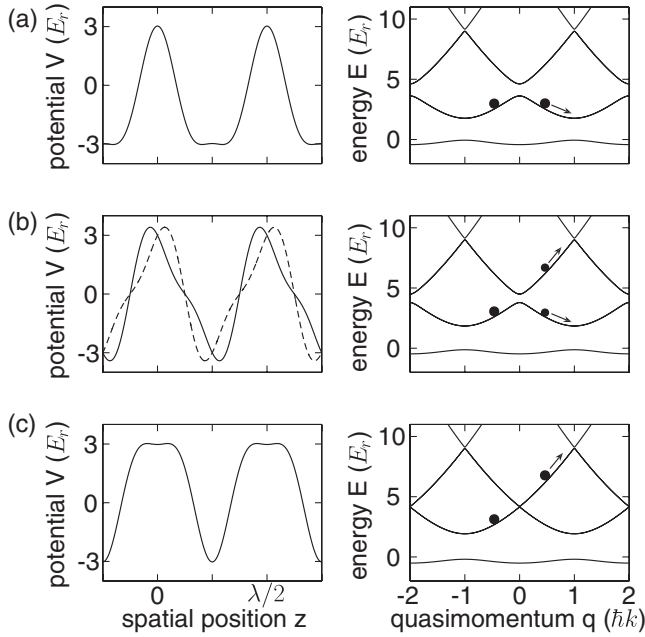


FIG. 1. Spatial potential (left) and band structure (right) for a periodic atom potential $V(z) = V_1 \cos(2kz)/2 + V_2 \cos(4kz + \varphi)/2$ for different values of the phase φ between lattice harmonics: (a) $\varphi = 0^\circ$: periodic sequence of hills, (b) $\varphi = 90^\circ$ (solid line) and $\varphi = -90^\circ$ (dashed line): sawtooth-like potentials, (c) $\varphi = 180^\circ$: periodic sequence of dimples. Here, $V_1 = 4E_r$ and $V_2 = 1.2E_r$ were used for the sake of clarity as an example for a set of potential values in which the splitting between first and second excited Bloch band vanishes at $\varphi = 180^\circ$. The size of this band gap can be studied by Landau-Zener tunneling of atoms, as indicated in the plots.

gap reaches a maximum value for $\varphi = 0^\circ$ in which case the lattice potential resembles a periodic sequence of hills [Fig. 1(a)]. On the other hand, the band gap reaches its minimum value for $\varphi = 180^\circ$, corresponding to an array of potential dimples in the spatial lattice structure [Fig. 1(c)]. For a suitable choice of potential values, the band gap between first and second excited band can even disappear. The situation of spatial lattice potentials with broken spatial symmetry, as, e.g., the sawtooth-like structures shown in Fig. 1(b) for $\varphi = \pm 90^\circ$, yields an intermediate value of the band gap.

We experimentally exploit the band structure of the Fourier-synthesized lattice by means of quantum transport experiments. Specifically, the size of the gap between first and second excited Bloch bands is measured by means of Landau-Zener tunneling of atoms in an accelerated lattice potential. The acceleration provides an inertial force in the moving lattice frame, emulating a force on atomic wave packets. The Landau-Zener tunneling probability can be estimated to be $\Gamma = \exp(-a_c/a)$, where $a_c = \pi\Delta^2/(4\hbar^2k)$ with Δ denoting the width of the energy gap.

Our method for generating a lattice potential with variable spatial symmetry and form is similar as described previously [10]. For the generation of the fundamental frequency, we use a conventional standing wave lattice

potential, as achieved with two counterpropagating optical waves with frequency ω detuned from an atomic resonance. The resulting potential $V(z) = -(\alpha/2)|E(z)|^2$, where α denotes the dynamic atomic polarizability and $E(z)$ the electric field, is proportional to $\cos^2 kz = (1 + \cos 2kz)/2$, yielding the well known $\lambda/2$ spatial periodicity of optical standing waves. In a quantum picture, the atoms undergo virtual two-photon processes of absorption of a photon from one mode followed by stimulated emission into the counterpropagating mode. In principle, a potential with periodicity $\lambda/4$ could be achieved by replacing the absorption and the stimulated emission cycle by a four-photon process induced by photons of wavelength λ , as indicated in Fig. 2(a) (right). The spatial periodicity of the achieved multiphoton lattice contribution is $\lambda_{\text{eff}}/2 = \lambda/4$, where $\lambda_{\text{eff}} = \lambda/2$ denotes the effective wavelength of a two-photon field. Figure 2(b) shows the used scheme for a multiphoton lattice potential with periodicity $\lambda/4$, which is based on a three-level configuration with two stable ground states $|g_0\rangle$ and $|g_1\rangle$ and one spontaneously decaying excited state $|e\rangle$ [11,12]. Compared to the four-photon ladder scheme, in this improved approach one absorption (stimulated emission) process has been replaced by a stimulated emission (absorption) process of a counterpropagating photon, respectively. A minimum of three laser frequencies is required to suppress standing wave effects, and the atoms are irradiated with two optical beams of frequencies $\omega + \Delta\omega$ and $\omega - \Delta\omega$ from one side and a further beam of frequency ω from the counterpropagating direction. The high frequency resolution of Raman spectroscopy here allows to clearly separate in frequency space the desired four-photon process from lower order contributions. The described scheme can be extended to higher lattice periodicities, where in general an effective potential with periodicity $\lambda/2n$ can be achieved by a $2n$ th order process [12]. By combining lattice potentials of different spatial periodicities, arbitrarily shaped periodic potentials can be synthesized.

Our experimental setup has been described in [10,13]. Briefly, light for generation of variable atomic lattice po-

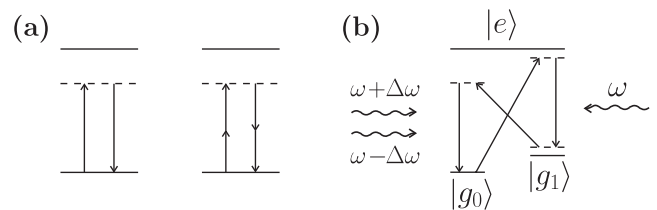


FIG. 2. (a) Left: Virtual two-photon process in a conventional standing wave lattice with $\lambda/2$ spatial periodicity. Right: Virtual process contributing to a lattice potential with $\lambda_{\text{eff}}/2 = \lambda/4$ periodicity in a ladder level scheme. However, unwanted standing wave effects dominate in this simple approach. (b) Improved configuration for realization of a four-photon lattice with $\lambda/4$ spatial periodicity. This scheme is used in our experiments to generate a second spatial lattice harmonic.

tentials is produced by a tapered diode laser tuned some 2 nm to the red of the rubidium $D2$ line. The emitted radiation is split into two, and each of the partial beams pass an acousto-optic modulator. The modulators are used for beam switching and to superimpose several optical frequencies onto a single beam path, as is required to generate superpositions of a standing wave potential and a four-photon lattice potential by realizing the scheme of Fig. 2(b). After passing the modulators, the two beams are directed through optical fibers and send in a counterpropagating geometry onto a rubidium (^{87}Rb) Bose-Einstein condensate.

Our Bose-Einstein condensate is produced all-optically by evaporative cooling of ^{87}Rb atoms in a CO_2 -laser dipole trap. During the evaporation, a magnetic field gradient is activated, resulting a spin-polarized condensate with 1.6×10^4 atoms in the $|F = 1, m_F = -1\rangle$ ground state. A magnetic bias field generates a frequency splitting of $\omega_z \approx 2\pi \times 805$ kHz between neighboring Zeeman ground states. The direction of the magnetic field forms an angle, respectively, to the optical beam, so that atoms experience σ^+ , σ^- and π -polarized light simultaneously. For generation of a multiphoton lattice potential with the scheme of Fig. 2(b), the $F = 1$ ground state components $m_F = -1$ and 0 are used as states $|g_0\rangle$ and $|g_1\rangle$, while the $5P_{3/2}$ -manifold serves as the excited state $|e\rangle$. The Raman detuning δ is $2\pi \times 50$ kHz. The used potential depths are $V_1 \approx 3E_r$ and $V_2 \approx 2E_r$ for the lattice contributions with periodicities $\lambda/2$ and $\lambda/4$, respectively, and different values of the phase φ between the two spatial harmonics were used in the course of the experiments. Experimentally, the potential values of both lattice harmonics and the phase φ can be monitored by a series of Raman-Nath diffraction experiments on pulsed optical potentials and Rabi oscillations [10,14], so that all parameters of the Fourier-synthesized lattice potential of Eq. (1) are known. One of the lattice beams with frequency ω is used for both the standing wave and the four-photon lattice potential. When this beam is acousto-optically detuned by a small amount δ_{Dopp} , the reference frame in which the optical potential is stationary moves with a velocity $v_{\text{rel}} = \delta_{\text{Dopp}}/2\pi \cdot \lambda/2$, where λ denotes the laser wavelength. We adiabatically load the atomic Bose-Einstein condensate into the first band by transferring the atoms into a lattice potential moving with $v_{\text{rel}} \equiv q_0/m \approx 1.5\hbar k/m$.

The lattice beams form an angle of 41° relatively to the axis of gravity, and the ballistic free atomic fall accelerates the atoms over the band gap between the first and second excited Bloch band. Figure 3 shows the result of a measurement monitoring for different final values of the atomic quasimomentum. Here, two different lattice forms were investigated. For a phase shift $\varphi \approx 0^\circ$ (dots), corresponding to a potential form with a sequence of hills, atoms are Bragg diffracted at the band gap towards higher velocities. In contrast, for a phase shift $\varphi \approx 180^\circ$ (crosses), corresponding to a lattice consisting of a periodic sequence of

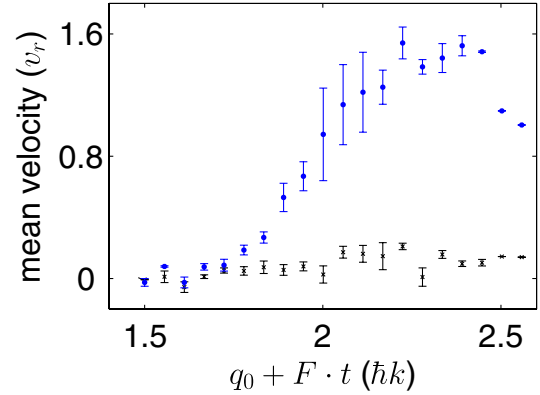


FIG. 3 (color online). Temporal variation of the mean atomic velocity in units of the recoil velocity ($v_r = \hbar k/m$) for an atom with initial momentum of $q_0 = 1.5\hbar k$ subject to the earth's gravitational field and the lattice potential for a phase φ of 0° (dots) and 180° (crosses) between lattice harmonics. The earth's gravitational force along the lattice axis is $F = mg \cos\alpha$, where $\alpha \approx 41^\circ$.

dimples, the ballistic free atom flight is hardly modified by a band gap between the first two excited bands. We attribute this striking modification of transport properties on the potential shape to the strong dependence of the size of the band gap between the first two excited Bloch bands on the relative phase φ between lattice harmonics. For a phase shift $\varphi = 180^\circ$, almost all atoms undergo Landau-Zener transitions over the band gap near $q = 2\hbar k$ (corresponding to the second gap at $q = 0$ in the reduced zone scheme), while adiabaticity is better achieved with $\varphi = 0^\circ$, giving evidence for an increased splitting of the band gap. At the band gap, Bragg diffraction changes the atomic momentum in units of $4\hbar k$.

For a more detailed investigation of the band gap we have recorded the Landau-Zener tunneling rate as a function of the phase between the lattice harmonics. For this measurement we have increased the beam detuning δ_{Dopp} with a constant rate, so that the lattice potential is accelerated relatively to the atomic frame with an acceleration of 6.44 m/s^2 , somewhat exceeding the projection of the Earth's gravitational field onto the beam axis. Figure 4 shows experimental data for the fraction of tunneled atoms as a function of phase φ between the two lattice harmonics. The data fit well to a sinusoidal curve, as shown by the solid line. Notably, asymmetrically shaped ratchetlike potentials result in an intermediate value of the Landau-Zener tunneling rate, while smallest (largest) values are achieved for hill-type (dimple-type) periodic arrays. It is interesting to note that this characteristics is in contrast to the behavior in dissipative lattices, where maxima and minima of the particle transport are achieved for ratchetlike potentials of different symmetry. Experimentally, a related observation has been made in pulsed, driven ratchet potentials [7].

In subsequent experiments, we have studied the variation of the Landau-Zener tunneling rate on the depth of the optical standing wave contribution to the total optical

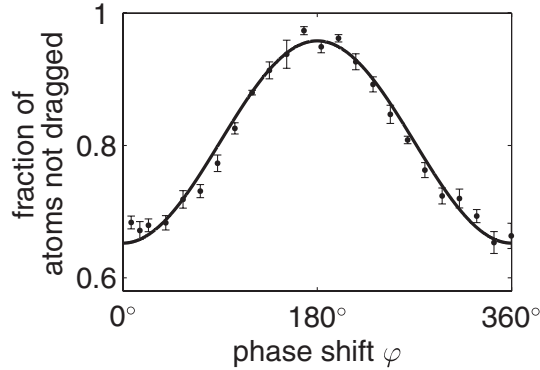


FIG. 4. Fraction of atoms that have tunneled through the energy gap between first and second excited Bloch bands as a function of phase φ between spatial lattice harmonics. The experimental data (dots) has been fitted with a sinusoidal curve (solid line).

potential. The four-photon contribution with periodicity of $\lambda/4$ here was left constant [see Eq. (1)]. Figure 5 shows experimental data for the interband tunneling for a phase shift $\varphi = 0^\circ$ (dots) and $\varphi = 180^\circ$ (crosses). For the former phase shift value, the tunneling rate decreases with the standing wave contribution V_1 for all parts of the curve, as is consistent with a monotonely increasing energy gap between the bands. On the other hand, for a phase shift $\varphi = 180^\circ$ between lattice harmonics a local maximum of the tunnelling rate is observed for an intermediate value of V_1 . This is attributed to the width of the band gap between the lowest two excited bands reaching a minimum for certain value of V_1 , as is expected when considering that the band gap for this phase shift value is diminished by destructive interference of the amplitudes of second order Bragg scattering of the standing wave potential and first

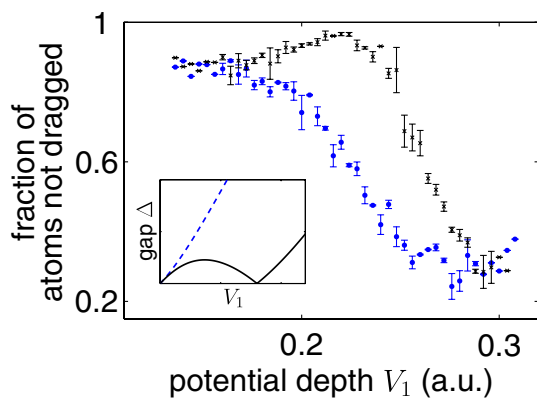


FIG. 5 (color online). Fraction of atoms that have tunneled from the first to the second excited band as a function of the potential depth V_1 of the standing wave contribution to the total lattice potential for a phase $\varphi = 0^\circ$ (dots) and $\varphi = 180^\circ$ (crosses) between lattice harmonics. The inset indicates the variation of the expected gap size on V_1 for $\varphi = 0^\circ$ (dashed line) and $\varphi = 180^\circ$ (solid line).

order Bragg scattering of the potential with periodicity $\lambda/4$. The inset of Fig. 5 is to indicate the dependence of the theoretical value of the band gap as a function of V_1 . We interpret the experimental data of Fig. 5 as clear evidence for the destructive (constructive) interference of scattering amplitudes contributing to the size of the band gap at a phase shift of $\varphi = 180^\circ$ ($\varphi = 0^\circ$), respectively, between lattice harmonics.

To conclude, we have studied the band structure of optical lattices with variable spatial symmetry and shape by means of quantum transport of an atomic Bose-Einstein condensate. We find that the Landau-Zener tunneling rate between the first and second excited Bloch band depends critically on the phase between spatial Fourier components of the lattice, which is attributed to interference effects within the band spectrum.

For the future, we expect that optical lattices of non-standard shape allow for novel quantum gas phases, and model solid state physics problems such as quantum magnetism and frustrated lattices [15–17]. A different perspective includes quantum ratchets with atomic Bose-Einstein condensates [18]. An exploration of the Hamiltonian ratchet regime is expected to allow for novel quantum dynamical phenomena.

We thank P. Hänggi for discussion in which the idea to study Landau-Zener tunneling in lattices of variable shape arose. We acknowledge financial support of the Deutsche Forschungsgemeinschaft.

- [1] See, e.g., C. Kittel, *Introduction to Solid State Physics* (John Wiley & Sons, New York, 1956).
- [2] See e.g.: I. Bloch, *Nature Phys.* **1**, 23 (2005).
- [3] M. Ben Dahan *et al.*, *Phys. Rev. Lett.* **76**, 4508 (1996).
- [4] Q. Niu, X.-G. Zhao, G. A. Georgakis, and M. G. Raizen, *Phys. Rev. Lett.* **76**, 4504 (1996).
- [5] C. F. Bharucha *et al.*, *Phys. Rev. A* **55**, R857 (1997).
- [6] J. P. Eisenstein *et al.*, *Phys. Rev. Lett.* **53**, 2579 (1984).
- [7] R. Gommers, S. Bergamini, and F. Renzoni, *Phys. Rev. Lett.* **95**, 073003 (2005).
- [8] B. M. Breid, D. Witthaut, and H. J. Korsch, *New J. Phys.* **9**, 62 (2007).
- [9] F. Bloch, *Z. Phys.* **52**, 555 (1928).
- [10] G. Ritt *et al.*, *Phys. Rev. A* **74**, 063622 (2006).
- [11] P. R. Berman, B. Dubetsky, and J. L. Cohen, *Phys. Rev. A* **58**, 4801 (1998).
- [12] M. Weitz, G. Cennini, G. Ritt, and C. Geckeler, *Phys. Rev. A* **70**, 043414 (2004).
- [13] G. Cennini, G. Ritt, C. Geckeler, and M. Weitz, *Phys. Rev. Lett.* **91**, 240408 (2003).
- [14] A. S. Mellish, G. Duffy, C. McKenzie, R. Geursen, and A. C. Wilson, *Phys. Rev. A* **68**, 051601(R) (2003).
- [15] B. Damski *et al.*, *Phys. Rev. Lett.* **95**, 060403 (2005).
- [16] L.-M. Duan, E. Demler, and M. D. Lukin, *Phys. Rev. Lett.* **91**, 090402 (2003).
- [17] L. Santos *et al.*, *Phys. Rev. Lett.* **93**, 030601 (2004).
- [18] S. Denisov, L. Morales-Molina, S. Flach, and P. Hänggi, *Phys. Rev. A* **75**, 063424 (2007).